

Impedance spectroscopic estimation of inter-granular phase distribution in 15 mol% calcia-stabilized zirconia/alumina composites

Jong-Heun Lee*, Toshiyuki Mori, Ji-Guang Li, Takayasu Ikegami, Satoshi Takenouchi

National Institute for Research in Inorganic Materials, Namiki 1-1, Tsukuba, Ibaraki, 305-0044, Japan

Received 8 March 2000; received in revised form 10 May 2000; accepted 26 May 2000

Abstract

The distribution of inter-granular glass phase in 15 mol% calcia-stabilized zirconia containing 0.3 or 10 μm size Al_2O_3 was estimated using a series of complex impedance spectra attained by successive removal of outer layers and subsequent measurements. For the instance of fine Al_2O_3 addition, the grain boundary at the near-surface region became more resistive than that at the center when sintered at $T \geq 1550^\circ\text{C}$, which emanated from the outward expelling of inter-granular phase during grain growth. In comparison, the coarse Al_2O_3 addition showed the homogeneous distribution of grain-boundary resistivity (ρ_{gb}). The ρ_{gb} as a function of sample depth could be an effective and sensitive index for determining the distribution of inter-granular phase. © 2000 Elsevier Science Ltd. All rights reserved.

Keywords: Impedance spectroscopy; Ionic conductivity; Grain boundaries; ZrO_2

1. Introduction

The siliceous inter-granular phase is known to deteriorate grain-boundary conduction of stabilized zirconia,^{1,2} the representative solid electrolyte. So far, Al_2O_3 was reported as the most effective scavenger for neutralizing harmful grain-boundary phase.^{2–4} However, there were also contradictory reports.⁵

Godickemeier et al.⁶ reported that the grain-boundary conductivity of Y_2O_3 tetragonal zirconia polycrystal (3Y-TZP) with Al_2O_3 addition is closely related with the co-existing SiO_2 amount. The formation of inter-granular glass phase was suggested as a key feature. The present authors also reported the two different roles of Al_2O_3 in grain-boundary conduction at 15 mol% calcia-stabilized zirconia (15CSZ).⁷ One is the improvement by scavenging reaction when sintered at $T \leq 1500^\circ\text{C}$ and the other is the deterioration by forming harmful inter-granular glass phase due to Al_2O_3 dissolution at $T > 1550^\circ\text{C}$. The grain-boundary conduction deteriorated more by the addition of 10 μm size single crystal-

line Al_2O_3 rather than by that of fine Al_2O_3 powder at 1600°C .

The improvement of grain-boundary conduction in stabilized zirconia by the addition of Al_2O_3 , therefore, should be understood in the framework of inter-granular glass phase unless the materials were extremely pure. It includes the change in the wetting behavior, distribution, and rearrangement of inter-granular glass phase. In this study, the distribution and the rearrangement of inter-granular phase were estimated in 15CSZ containing 0.3 or 10 μm size Al_2O_3 . A series of complex impedance spectra was attained from the successive removing of outer layers by polishing and subsequent measurement. The grain-boundary resistance as a function of sample depth was analyzed in relation to the distribution of inter-granular phase.

2. Experimental procedure

The 15CSZ powders (CSZ-15 Heat-treated, Daiichi Kigenso Kagaku Kogyo Co. Ltd., Osaka, Japan) were used as raw material. The concentrations of the impurities SiO_2 , TiO_2 , FeO_3 , and Na_2O were quoted as 0.05, 0.11, 0.023, and 0.02 wt.%. The 1 mol% of Al_2O_3

* Corresponding author. Tel.: +81-298-51-3354, ext. 2247; fax: +81-298-52-7449.

E-mail address: jongheun@yahoo.com (J.-H. Lee).

Table 1
The specifications, source materials, sintering conditions, densities and average grain sizes of the samples

Sample	Source materials	Sintering	Density ^a (g/cm ³)	d _g ^b (μm)
15CSZ-1A ₁₀ -1600	15CSZ + 1 mol% Al ₂ O ₃ (10 μm)	1600°C, 4 h	5.44	40.7
15CSZ-1A ₀₃ -1600	15CSZ + 1 mol% Al ₂ O ₃ (0.3 μm)	1600°C, 4 h	5.50	38.9
15CSZ-1A ₀₃ -1550	15CSZ + 1 mol% Al ₂ O ₃ (0.3 μm)	1550°C, 4 h	5.47	25.5
15CSZ-1A ₀₃ -1500	15CSZ + 1 mol% Al ₂ O ₃ (0.3 μm)	1500°C, 4 h	5.47	17.2

^a Apparent densities measured by Archimedes' method.

^b Average grain sizes of more than 500 grains determined by linear intercept method.

powder sized 0.3 μm (AKP30, Sumitomo Chemical Co., Tokyo, Japan) or the single crystalline Al₂O₃ particles sized 10 μm (AA10, Sumitomo Chemical Co., Tokyo, Japan) with mono-disperse distribution were added. Table 1 summarized the specifications, source materials, densities, and average grain sizes of the samples.

A combination of 15CSZ, Al₂O₃, and C₂H₅OH was vigorously stirred for 1 h with ultrasonic vibration for good dispersion. After removing the solvent by rotatory evaporator and drying, the soft aggregation was pulverized. About 2.2 g of powders were uniaxially pressed into pellet and then isostatically pressed at 200 MPa. The pellets were sintered at 1500–1600°C for 4 h in air atmosphere. The heating and cooling rates were fixed to 200°C/h. Platinum electrodes were applied to the pellet by coating of Pt paste (TR 7905, Tanaka Co., Tokyo, Japan), drying, and subsequent heat treatment at 1000°C for 1 h. The schematic sample dimension and electrode configurations were shown in Fig. 1. After each impedance measurement, 1/20 portions of original sample thickness (*t*) were polished away from both sides to obtain the spectra as a function of distance from the surface. The center part of sintered body was cut, polished and then thermally etched at 1400°C for 1 h for SEM observation. The complex impedance was measured using ac three-probe technique by SI 1260

impedance/gain-phase analyzer (Model No. SI 1260, Solartron, Inc., Farnborough, UK).

3. Results and discussion

Two sets of impedance spectra for 15CSZ-1A₀₃-1600 and 15CSZ-1A₁₀-1600 were measured with successive removing the outer regions. Fig. 2 show results. The series of three parallel RC sections was considered as an equivalent circuit. The semicircle at the low frequency regime was the contribution by electrode polarization, which was proved by comparing the several impedance spectra with the different sample thicknesses. The capacitance values for the RC rumps were calculated as about 7.6~11×10⁻⁹ F/cm for the middle-frequency region and about 4.4×10⁻¹² F/cm for the high-frequency one, if we assumed a Debye-type relaxation ($\omega\rho C=1$) where ω , ρ , and C are angular frequency, resistivity and capacitance, respectively. From the agreement of these values with those for grain boundary and grain interior in the literature,⁸ the semicircles at the middle and high frequencies were attributed to the contributions of grain boundary and grain interior, respectively.

The grain-boundary resistivity deconvoluted from impedance spectrum (ρ_{gb}) was smaller in 15CSZ-1A₀₃-1600 than in 15CSZ-1A₁₀-1600. It will be discussed later in this paper. The ρ_{gb} of 15CSZ-1A₀₃-1600 decreased systematically with the removal of outer layers [Fig. 2(a)], whereas that of 15CSZ-1A₁₀-1600 did not show any significant change [Fig. 2(b)]. This indicates that the outer part of 15CSZ-1A₀₃-1600 has a more resistive grain boundary than the inner regime.

Fig. 3 shows the microstructures of the cross-sections. There was no abnormal grain growth that can affect the analysis based on a brick-layer model.⁹ The inter-granular and intra-granular dark regions represent Al₂O₃ or that reacted with inter-granular phase. At 1500°C, both pointy and elongated dark regions can be found [Fig. 3(d)]. Almost all of them changed into elongated morphologies along the grain boundary at 1600°C [Fig. 3(c)], which means Al₂O₃ dissolution into inter-granular glass phase. The main components that constitute inter-

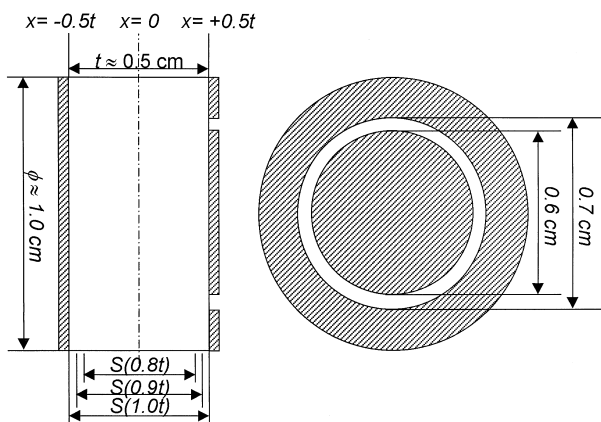


Fig. 1. The schematic sample dimension and electrode configuration of a sample for impedance measurement.

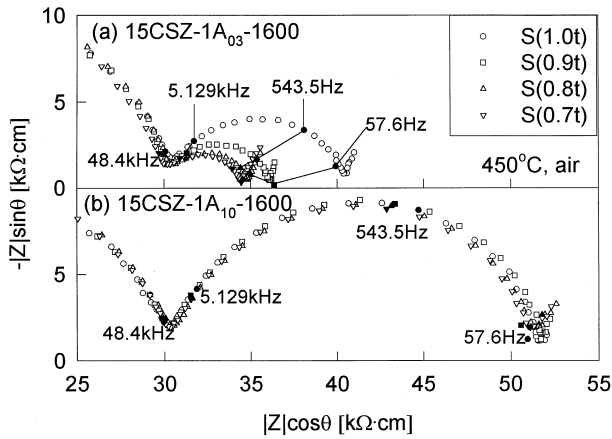


Fig. 2. The impedance spectra of 15CSZ-1A₀₃-1600 and 15CSZ-1A₁₀-1600 at 450°C in air measured after successive removal of 1/20 portions of the original sample thickness (*t*) from both outer regions, respectively (see the notations in Fig. 1).

granular phase were considered as CaO, SiO₂, and Al₂O₃ from the literatures on the grain-boundary segregation in CSZ^{1,10} and from the former investigation.⁷ The pores A and B in Fig. 3(a) sized about 10 μm were proved as the sites that had been fully occupied by Al₂O₃ particles at low temperatures. The pore partly occupied by small Al₂O₃ particles [B in Fig. 3(a)] supports the dissolution of coarse Al₂O₃ particles into intergranular phase. It was difficult to find the distinct changes of grain sizes and morphologies between the outer region [near *x* = 0.5*t*, arrowed in Fig. 3(b)] and the center (near *x* = 0) for all the samples. No notable

microstructural change, notwithstanding heterogeneous ρ_{gb} distribution, therefore indicates that the SEM observation is insufficient to investigate the distribution of inter-granular phase in the present study.

For further information, the heterogeneity of ρ_{gb} in 15CSZ-1A₀₃ sintered at 1500 and 1550°C was checked. The results are shown in Fig. 4 with those of 15CSZ-1A₀₃-1600 and 15CSZ-1A₁₀-1600. A small difference between the outermost and center layers was found at 1550°C and then vanished at 1500°C. In order to check the siliceous contamination from the furnace at the higher temperature, the 15CSZ-1A₀₃ pellet was surrounded by the same composition of powder during sintering at 1600°C. The tendency of a more resistive layer at the outside was the same and there was bonding between the pellet and adjacent powder. This suggests that the resistive layer at the outermost regime resulted not from contamination during sintering but from redistribution of the inter-granular liquid phase that begins at about 1550°C. The ρ_{gb} value in Fig. 4 is the cumulative one. From the lack of substantial variations in grain size with sample depth, one can assume the same number of grain boundaries per unit length for the entire portions. Therefore, ρ_{gb} of the outermost part [ρ_{gb} (outermost)] can be calculated by the following equation

$$\begin{aligned} &\rho_{gb}[S(0.9t)] \cdot 0.9t + \rho_{gb}(\text{outermost}) \cdot 0.1t \\ &= \rho_{gb}[S(1.0t)] \cdot 1.0t \end{aligned} \quad (1)$$

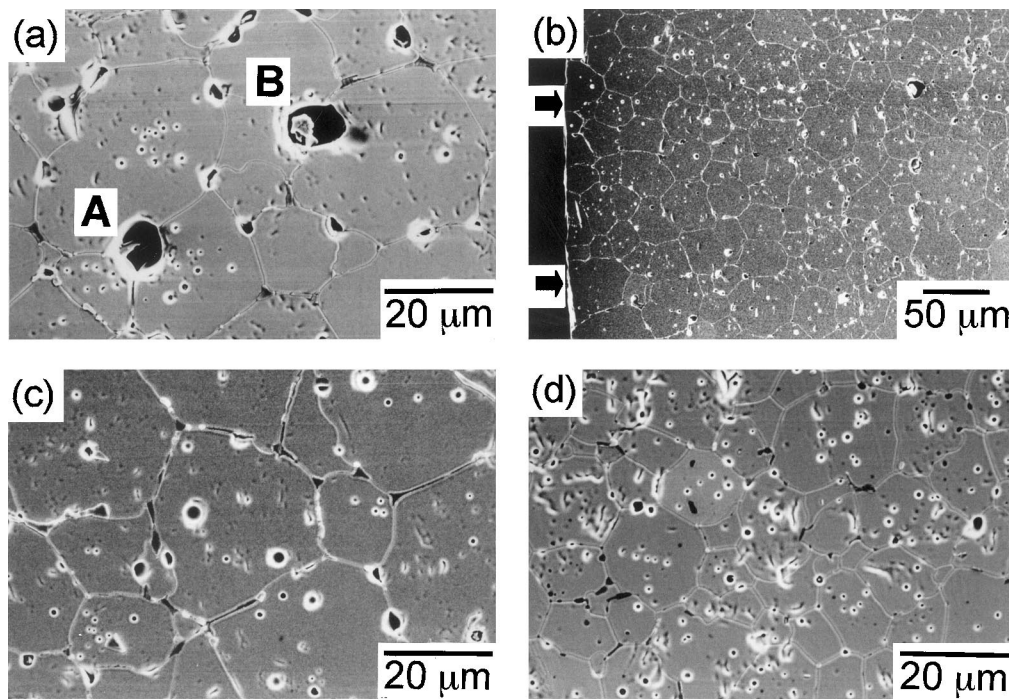


Fig. 3. Scanning electron micrographs of the sample cross-sections: (a) 15CSZ-1A₁₀-1600; (b) the cross-section of near surface region in 15CSZ-1A₀₃-1600 (near *x* = 0.5*t* in Fig. 1); (c) 15CSZ-1A₀₃-1600; and (d) 15CSZ-1A₀₃-1500.

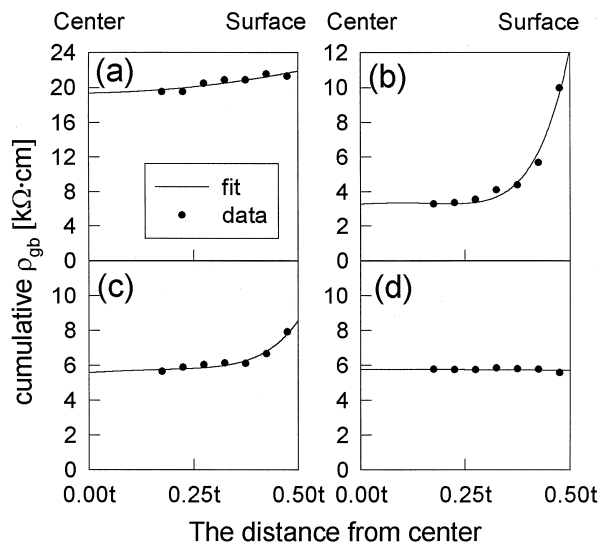


Fig. 4. Cumulative grain boundary resistivity (ρ_{gb}) at 450°C as a function of sample thickness: (a) 15CSZ-1A₁₀-1600; (b) 15CSZ-1A₀₃-1600; (c) 15CSZ-1A₀₃-1550; (d) 15CSZ-1A₀₃-1500.

where $\rho_{gb}[S(0.9t)]$, $\rho_{gb}[S(1.0t)]$, t are the ρ_{gb} of the samples $S(0.9t)$ and $S(1.0t)$ and original sample thickness, respectively (see the notation in Fig. 1). The $\rho_{gb}(\text{outermost})$ was calculated as 48.6 k Ω cm, which is about 14.8 times of $\rho_{gb}[S(0.4t)]$, 3.28 k Ω cm. As suggested in liquid phase sintering mechanism.¹¹ Inter-granular glass phase can be rearranged strongly toward the outside by the capillary force when the grain growth has occurred. Therefore, the outward rearrangement of inter-granular phase could be regarded as the origin for the resistive grain boundary at the outer region in 15CSZ-1A₀₃-1600.

About 15-fold increase of ρ_{gb} at the outer part can emanate for the following two reasons. One is the thickening of the grain-boundary glass phase. The specific grain-boundary resistivity (ρ_{gb}^{sp}) is given by the following equation:¹

$$\rho_{gb}^{sp} = \rho_{gb}(d_g/\delta_{gb}) \quad (2)$$

where d_g and δ_{gb} are average grain size and grain-boundary thickness, respectively. If δ_{gb} increased, ρ_{gb} would increase proportionally. Clarke suggested that the grain boundary usually has a finite thickness due to the balance between the attractive van der Waals force between the grains and 1-nm scale repulsion as a resistance to deformation of silicate glass structures.¹² Nevertheless, the thickening of the grain boundary cannot be excluded because the above suggestion cannot explain the instance of a large liquid portion and because the force balance can be changed at the near-surface regions. For example, Chaim et al. studied the surface segregation of Fe-rich silicate glass phase in 4

wt.% Y₂O₃-TZP.¹³ They observed the thicker grain boundary in the surface region using TEM. It reflects that the thickening of the grain boundary can increase ρ_{gb} in this study. The other is the more homogeneous distribution of inter-granular phase at the near-surface region due to its abundance, which can make the grain-boundary conduction more difficult. Both these reasons can be considered applicable.

The ρ_{gb} of 15CSZ-1A₁₀-1600 is larger than that of 15CSZ-1A₀₃-1600. The scavenging effect by 10 μm size Al₂O₃ was almost the same, or better, than that by 0.3 μm size Al₂O₃ at 1450–1500°C. Hence, the insufficient scavenging of resistive grain-boundary phase due to the small number of coarse Al₂O₃ particles was excluded. Another important parameter is the distribution of liquid phase. For fine Al₂O₃ addition, the aforementioned outward expelling of liquid phase made heterogeneous ρ_{gb} distribution at $T \geq 1550^\circ\text{C}$. This temperature agrees well with the starting of the complete Al₂O₃ dissolution into inter-granular phase in the previous report.⁷ However, for the instance of 15CSZ-1A₁₀-1600, there still remains unreacted Al₂O₃ [see B Fig. 3(a)]. From the phase diagram in CaO–SiO₂–Al₂O₃,¹⁴ the lower Al₂O₃ content tends to form the liquid phase at the higher temperatures although there are many possible glass compositions. It implies that the outward redistribution of glass phase is not probable in 15CSZ-1A₁₀-1600. Furthermore, the compositional difference in CaO–SiO–Al₂O₃ could accompany the change in viscosity and wetting behavior of liquid phase. A combination of the above reasons was understood as the origin for the homogeneous and higher ρ_{gb} of 15CSZ-1A₁₀-1600 rather than that of 15CSZ-1A₀₃-1600.

4. Conclusions

The grain-boundary contributions in a series of complex impedance spectra attained by successive removing outer layers were correlated with the distribution and rearrangement of inter-granular glass phase in 15CSZ containing Al₂O₃. The grain boundary at the outermost portion becomes about 15 times more resistive than that at the inner region as sintering temperatures increased to 1600°C when fine Al₂O₃ was added. This indicates the outward rearrangement of liquid phase with increasing temperatures. In stabilized zirconia, the grain-boundary resistivity could be an effective tool to estimate inter-granular glass phase.

Acknowledgements

One of the authors, J.-H.L. thanks JISTEC/JST of Japan for an STA fellowship.

References

1. Aoki, M., Chiang, Y.-M., Kosacki, I., Lee, J.-R., Tuller, H. and Liu, Y., Solute segregation and grain-boundary impedance in high purity stabilized zirconia. *J. Am. Ceram. Soc.*, 1996, **79**, 1169–1180.
2. Lee, J.-H., Mori, T., Li, J.-G., Ikegami, T., Komatsu, M. and Haneda, H., Imaging secondary ion mass spectroscopy observation of the scavenging of siliceous film from 8 mol% yttria-stabilized zirconia by the addition of alumina. *J. Am. Ceram. Soc.* 2000, **83**, 1273–1275.
3. Feighery, A. J. and Irvine, J. T. S., Effect of alumina additions upon electrical properties of 8 mol.% yttria-stabilized zirconia. *Solid State Ionics*, 1999, **121**, 209–216.
4. Rajendran, S., Drennan, J. and Badwal, S. P. S., Effect of alumina additions on the grain boundary and volume resistivity of tetragonal zirconia polycrystals. *J. Mater. Sci. Lett.*, 1987, **6**, 1431–1434.
5. Miyayama, M., Yanagida, H. and Asada, A., Effect of Al_2O_3 addition on resistivity and microstructure of yttria-stabilized zirconia. *Am. Ceram. Soc. Bull.*, 1986, **65**, 660–664.
6. Godickemier, M., Michel, B., Orliukas, A., Bohac, P., Sasaki, K. and Gauckler, L., Effect of intergranular glass films on the electrical conductivity of 3Y-TZP. *J. Mater. Res.*, 1994, **9**, 1228–1240.
7. Lee, J.-H., Mori, T., Li, J.-G., Ikegami, T. and Takenouchi, S., The influence of alumina addition and its distribution upon grain-boundary conduction in 15 mol% calcia-stabilized zirconia. *Ceramics International*, in press.
8. Bonanos, N., Slotwinski, R. K., Steele, B. C. H. and Butler, E. P., Electrical conductivity/microstructural relationships in aged CaO and CaO+MgO partially-stabilized zirconia. *J. Mater. Sci.*, 1984, **19**, 785–797.
9. Fleig, J. and Maier, J., The impedance of ceramics with highly resistive grain boundaries: validity and limits of the brick layer model. *J. Eur. Ceram. Soc.*, 1999, **19**, 693–696.
10. Shackelford, J. F., Nicholson, P. S. and Smeltzer, W. W., Influence of SiO_2 on sintering of partially stabilized zirconia. *Am. Ceram. Soc. Bull.*, 1974, **53**, 865–867.
11. Souza, D. P. F. De and Souza, M. F. De, Liquid phase sintering of RE_2O_3 : YSZ ceramics: part I, grain growth and expelling of the grain boundary glass phase. *J. Mater. Sci.*, 1999, **34**, 4023–4030.
12. Clarke, D. R., On the equilibrium thickness of intergranular glass phases in ceramic materials. *J. Am. Ceram. Soc.*, 1987, **70**, 15–22.
13. Chaim, R., Brandon, D. G. and Heuer, A. H., A diffusional phase transformation in ZrO_2 -4wt% Y_2O_3 induced by surface segregation. *Acta Metall.*, 1986, **34**, 1933–1939.
14. Chiang, Y.-M., Birnie, D. P. III and Kingery, W. D., *Physical ceramics*. John Wiley & Sons Inc, New York, 1997 p. 332.